Inorg. Chem. **2004**, *43*, 1411−1420

Calculation of the Ground and Excited States of a Mixed Valence Compound $[Fe_2(OH)_3(NH_3)_6]^{2+}$: A Class II or Class III Compound?

Yannick Carissan,* Jean-Louis Heully, Fabienne Alary, and Jean-Pierre Daudey

Laboratoire de Physique Quantique, IRSAMC, Université Paul Sabatier, 118, Route de Narbonne, 31062 Toulouse Cedex, France

Received June 23, 2003

The effective group potentials (EGP) approach has been successfully used for the computation of the ground and excited states energies of the mixed valence compound $[Fe_2(OH)_3(NH_3)_6]^{2+}$. It is the first time that for a system as big as the complex presented above the ground and excited states are computed with their own orbitals and studied in such a detailed way. First of all, the NH_3 EGP was validated by comparing calculations where NH_3 was treated explicitly at different levels of calculations. Once the validation was obtained, the complete spectrum of the compound under interest was calculated and compared with results obtained in a previous work by Barone et al. and the spin Hamiltonian of widespread use. Some deviations from these predictive approaches were observed. This allowed us to emphasize the importance of the dynamic correlation which is not included explicitly in the spin Hamiltonian. Then, the influence of vibration has been studied by computing the potential energy curves obtained when moving the $(OH)_3$ plane. This study shows that our calculations lead to a delocalized compound (class III) as expected according to former experimental data.

1. Introduction

A molecule (charged or not) with two transition metal atoms containing an odd number of electrons is a challenge for a theoretical chemist. The challenge is even more interesting if the open shell is delocalized over the two centers. In this specific case, it is called a mixed valence compound. One has three different ways of describing the electronic configuration of the molecule depending on the delocalization of the extra electron. This classification was first introduced by Robin and Day.[23] The first one is to say that the electron is localized on one metallic center. In that case the oxidation numbers of the two metals are different.

* To whom correspondence should be addressed. E-mail: yannick.carissan@irsamc.ups-tlse.fr.

(1) Alary, F.; Poteau, R.; Heully, J.-L.; Barthelat, J.-C.; Daudey, J.-P. *Theor. Chem. Acc.* **2000**, *104*, 174−178.
(2) Poteau, R.; Ortega, I.; Alary, F.; Solis, A. R.; Barthelat, J.-C.; Daudey, J.-P. *J. Phys. Chem. A* **2001**, *105*, 198−205.
(3) Poteau, R.; Alary, F.; Abou El Makarim, H.; Heully, J.-L.; Barthelat, J.-C.; Daudey, J.-P. *J. Phys. Chem. A* **2001**, *105*, 206−214.
(4) Heully, J.-L.; Poteau, R.; Berasaluce, S.; Alary, F. *J. Chem. Phys.* **2002**, *116*, 4829−4836.
(5) Barone, V.; Bencini, A.; Ciofini, I.; Daul, C. A.; Totti, F. *J. Am. Chem. Soc.* **1998**, *120*, 8357−8365.
(6) Ding, X. Q.; Bominaar, E. L.; Bill, E.; Winkler, H.; Trautwein, A. X. *J. Chem. Phys.* **1990**, *92*, 178−186.
(7) Kahn, O. *Molecular Magnetism*; VCH Publishers: New York, 1993.
(8) Froese Fischer, C. *The Hartree−Fock method for atoms*; Wiley-Interscience: New York, 1977.
(9) Helgaker, T.; Jørgensen, P.; Olsen, J. *Molecular Electronic-Structure Theory*; Wiley & Sons: New York, 2000.
(10) Dolg, M.; Wedig, U.; Stoll, H.; Preuss, H. *J. Chem. Phys.* **1987**, *86*, 866.
(11) Cundari, T. R.; Stevens, W. J. *J. Chem. Phys.* **1993**, *98*, 5555−5565.
(12) Bergner, A.; Dolg, M.; Kuechle, W.; Stoll, H.; Preuss, H. *Mol. Phys.* **1993**, *80*, 1431.
(13) Andersson, K. *Theor. Chim. Acta* **1995**, *91*, 31−46.
(14) Slater, J. C. *Quantum Theory of Molecules and Solids*; McGraw-Hill: New York, 1974.
(15) Gamelin, D. R.; Bominaar, E. L.; Kirk, M. L.; Wieghardt, K.; Solomon, E. I. *J. Am. Chem. Soc.* **1996**, *118*, 8085−8097.
(16) Blondin, G.; Girerd, J.-J. *Chem. Rev.* **1990**, *90*, 1359−1376.
(17) Schmidt, M. W.; Baldridge, K. K.; Boatz, J. A.; Elbert, S. T.; Gordon, M. S.; Jensen, J. H.; Koseki, S.; Matsunaga, N.; Nguyen, K. A.; Su, S. J.; Windus, T. L.; Dupuis, M.; Montgomery, J. A. *J. Comput. Chem.* **1993**, *14*, 1347−1363.
(18) Andersson, K.; Barysz, M.; Bernhardsson, A.; Blomberg, M. R. A.; Cooper, D. L.; Fleig, T.; Fülscher, M. P.; de Graaf, C.; Hess, B. A.; Karlström, G.; Lindh, R.; Malmqvist, P.-Å; Neogrády, P.; Olsen, J.; Roos, B. O.; Schimmelpfennig, B.; Schütz, M.; Seijo, L.; Serrano-Andrés, L.; Siegbahn, P. E. M.; Stålring, J.; Thorsteinsson, T.; Veryazov, V.; Widmark, P.-O. *MOLCAS Version 5*; Lund University: Sweden, 2000.
(19) Binkley, J. S.; Pople, J. A.; Hehre, W. J. *J. Am. Chem. Soc.* **1980**, *102*, 939−947.
(20) Angeli, C.; Cimiraglia, R.; Persico, M.; Toniolo, A. *Theor. Chem. Acc.* **1997**, *98*, 57−63.
(21) Angeli, C.; Persico, M. *Theor. Chem. Acc.* **1997**, *98*, 117−128.
(22) Finley, J.; Malmqvist, P.-Å.; Roos, B. J.; Serrano-Andrès, L. *Chem. Phys. Lett.* **1998**, *288*, 299−306.
(23) Robin, M. B.; Day, P. *Adv. Inorg. Chem. Radiochem.* **1967**, *10*, 247−403.

10.1021/ic034716h CCC: $27.50
Published on Web 01/28/2004

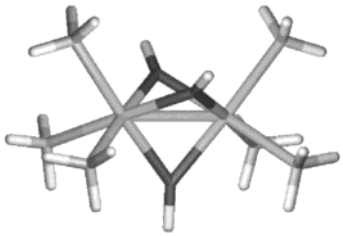

Figure 1. Representation of the $[Fe_2(OH)_3(NH_3)_6]^{2+}$ compound. Geometrical parameters taken from a previous work.[5]

The opposite one (the third one) is to delocalize the electronic structure completely. The oxidation numbers of the metallic centers being identical but nonintegers. The second one is an intermediate class which leads to a temperature dependent localization of the electron. The three classes mentioned above have been characterized experimentally.[6]

From a theoretical point of view the energy E of the different states of spin S was rationalized[7] using the following formula:

$$E(S, \pm) = \frac{J}{2}[S(S+1)] \pm B\left(S + \frac{1}{2}\right) \quad (1)$$

Before giving the meaning of the J and B constants, we shall focus on the $\pm$ sign. As mentioned above, the so-called extra electron can be localized on one center or the other one which we will refer for convenience as left and right. Then for a given total spin S, two states can be built. One with the electron localized on the left center and the other one with the electron on the right center. In a delocalized view, these two states correspond to symmetric or antisymmetric states with respect to the symmetry operation which transforms one metallic center to the other. If one analyzes eq 1, B represents the exchange of one electron between the two metallic centers. As a matter of fact, B is called the delocalization parameter. J is the superexchange isotropic constant. It is the parameter which lifts the degeneracy between states having the same spatial extension but a different total spin S.[7]

In a previous work by Barone et al.,[5] the mixed valence compound $[Fe_2(OH)_3(NH_3)_6]^{2+}$ (cf. Figure 1) has been studied using the broken symmetry approach with DFT calculations. This molecule was chosen to model the complex $[Fe_2(OH)_3(tmtacn)_2]^{2+}$ using NH_3 ligands to replace the tmtacn ligand (*N*,*N*′,*N*″-trimethyl-1,4,7-triazacyclononane). With these calculations, all excited states are not available except the lowest states within the irreducible representations of the symmetry group of the molecule. A comparison of theoretical and experimental studies of magnetic properties of molecular systems is summarized in a review presented by Ciofini and Daul.[24] We have decided to study this mixed valence compound because of the challenge it represents for a quantum chemist. We wanted to apply ab initio quantum mechanic methods at a high level of correlation and to compute the magnetic spectrum of this compound, which had not been done so far. Such a calculation does not appear feasible to a quantum chemist because of the difficulty a transition metal dimer represents and because of the size of the molecule but we managed to overcome these difficulties as explained later. Our aim in this study was twofold. First of all, we used EGP to reduce considerably the size of the system to treat which allowed us to be able to do CCSD (coupled cluster singles and doubles) and CASPT2 (complete active space self-consistent field with second-order perturbation theory). With such calculations, all the spectrum is thus in principle reachable. Therefore, we do not have to use the broken symmetry approach which makes the computation of the magnetic properties of this system (and others) easier. Second of all, once we have computed the spectrum at the CASPT2 level, we can compare our results to the spectrum we would obtain using eq 1 and test its validity on this specific system. Furthermore, we have computed the influence of a vibrational mode on the energy of the ground state ($E(^9/_2, -)$) and the highest localized state ($E(^1/_2, -)$) and compared it to the expected one.[7] To our knowledge this is the first time it is done at an ab initio level of calculation.

(24) Ciofini, I.; Daul, C. A. *Coord. Chem. Rev.* **2003**, *238*−*239*, 187−209.

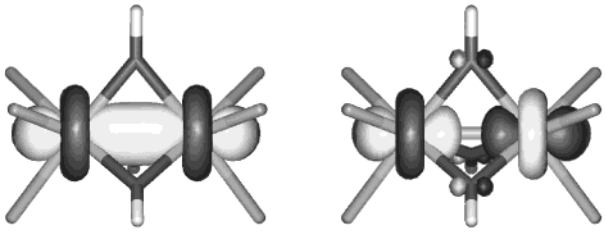

Figure 2. The bonding and antibonding orbitals under interest. The orbitals presented in this picture were obtained by a CASSCF calculation for the ground state of the molecule.

2. Presentation of the Problem

As stated in the Introduction, the work presented in this article aimed to compute the spectrum of a mixed valence molecule (Figure 1). Let us have a look in detail at the system and try to find an appropriate method to do this calculation in a reasonable time on a normal PC.

2.1. The scientific Challenge. 2.1.1. Physical Considerations. In order to understand the electronic structure of the mixed valence compound we are interested in, we shall focus on the Fe−Fe system which is the core of the magnetic properties of this system. In the mixed valence compound **1**, the two Fe atoms have formally two different oxidation numbers, +II and +III. This gives rise to an extra electron in the Fe−Fe system, i.e., 11 electrons in the 10 linear combinations of each set of five 3d orbitals. The ground state for this system is supposed to be in the spin multiplicity $2S + 1 = 10$. It is worth pointing out that the calculation of states with spin multiplicity higher than 4 is not common and is a real challenge. As stated in the Introduction, each state (S, −) differs from another state of the same spin multiplicity by the excitation of one electron from the bonding orbital to the antibonding one. The doubly occupied orbitals in these states are given in Figure 2. From the occupation of 10 orbitals with 11 electrons, states with spin multiplicity from 10 to 2 can arise. For each of these multiplicities, we propose computing two states which

correspond to the excitation of one electron from one molecular orbital mainly built on one iron to a molecular orbital mainly extended on the other iron, i.e., from the bonding orbital to the antibonding one. In order to compute these states properly, it is compulsory to take into account the fact that the wave function is multiconfigurational. In other words, such wave functions cannot be represented by one main configuration modified by some excitation. The representation has to be balanced; i.e., the weight of the configurations should have the possibility of being of the same order or equal. A general method to do the calculations with such restrictions is the CASSCF (complete active space self-consistent field) one. In a CASSCF approach, one distributes the electrons in an active orbital space, and one optimizes the molecular orbital coefficients and the weights of the configurations for each state. The choice of the active space is far from being trivial, and we shall discuss it in the next section. In our case, one should note that the number of configurations will increase rapidly as the spin decreases. By its definition given previously, the CASSCF method takes into account the fact that the wave function is multiconfigurational. It allows us to include the part of the correlation energy called the static correlation energy. In order to include the rest of the correlation energy, called the dynamic correlation energy, one should add the excitations which were not taken into account in the CASSCF wave function. Methods of choice would be MRCI methods, for instance, but the number of determinants increases so drastically that such a calculation is impossible. The CASPT2 method is a treatment of the single and double excitations on top of the CASSCF wave function in a perturbative approach only and thus is feasible.

2.1.2. Choice of the Active Space and Importance of the CASPT2 Treatment. In our study, the orbitals involved in the magnetic properties of the compound are the d orbitals of the Fe. Since we want to study the transitions between the states arising from the different occupations of these orbitals, our active space was chosen to be the 10 d orbitals occupied with 11 electrons. With this active space, we are able to generate all the excited states of interest. It would, perhaps, be better to follow the recommendation of Roos and of Pierloot and Froese Fisher[8] to include in the CAS two d orbitals per Fe (3d and 4d). The first one would introduce the correlation and the second one the polarization. But, since this would have increased the size of the calculation by too large a factor, we decided not to do so. We shall come back to this point in the next section.

Finally, the choice of the active space we took is also interesting since it includes precisely the effects which are taken into account in order to derive eq 1. The inclusion of the dynamic correlation will show whether this equation is still valid for a system with such a high spin or if some other effects due to the dynamic correlation have to be taken into account.

2.1.3. Note on Coupled Cluster and DFT. In this paper, we will give results of coupled cluster (CCSD) and DFT[5] calculations. These two methods do not fulfill the requirement of a balanced representation of the wave function. They are built on one determinant only and include the correlation energy in different ways. The CC includes the excitations (singles and double completely and some triples and quadruples) on top of the zero order wave function, whereas the DFT tries to include the entire correlation effect by means of a functional. However, the CC is suitable for the study of the wave functions which are mainly built on one determinant, in our case, the high spin of each symmetry. Concerning the lower spin states, this is not feasible anymore since one cannot represent them using one determinant. For this reason, the CCSD calculations were performed only on the high spin states.

Table 1. CPU Times[a] for the Same Calculation with and without EGPs

	ECPs only	ECPs + EGPs	gain
integrals	3058	1355	2.3
1 CASSCF iteration	10789	2915	3.7
1 CASPT2 iteration	3274	669	4.9

[a] In seconds.

2.2. The Size Problem Solved by the Use of EGPs. 2.2.1. Size Reduction. A general choice for production calculations would be to use effective core potentials on the metals, the nitrogens, and the oxygens and a small basis on the hydrogens. This choice (cf. section 3.1) would lead to 200 basis functions and 101 electrons. On the other hand one could use effective group potentials (cf. section 3.1) on the NH_3 ligands in order to reduce the size of the system. Then the number of primitive function and electrons drops from 200 to 158 and from 101 to 65, respectively.

Since our purpose is to compute the complete spectrum of the molecule, one would like to be able to use calculations methods such as coupled cluster or complete active space self-consistent field with the perturbation theory to take into account the dynamic correlation (CASSCF/CASPT2). According to Helgaker et al.,[9] the time-consuming step for CCSD scales such as n^6 and the time-consuming step of CASPT2 scales such as $n_{conf} \times n^5$. n is the number of basis functions, and n_{conf} is the number of configurations in the CASSCF wave function. With these numbers, the reduction factor for the computational time would be about 4.1 for a CCSD calculation and about 3.2 for a CASPT2 one. Note that these factors do not take into account the fact that the number of electrons treated explicitly is reduced by a factor $101/65 = 1.55$ which leads to a reduction of the number of excitations in the CCSD and CASPT2 wave functions. An example of CPU times for the calculation of the ground state at the CASPT2 level with or without EGP is given in Table 1. In this table are also presented the CPU times for the evaluation of the integrals. In this case, the improvement due to the presence of the EGPs is not as important as expected because in both calculations there is a threshold under which the integrals are assumed to be zero. So the number of evaluated integrals drops to 90899462 with ECPs and 37777606 (i.e., a ratio of 2.4) with EGPs. This is mainly due to the fact that in there is a non-negligible number of basis functions on the hydrogens of the NH_3 ligands which overlap loosely with the basis functions of the atoms at the opposite side of the molecule.

Table 2. Comparison of the Transitions[a] Obtained with 2 Different ECPs on the Fe Atoms and the NH_3 EGP

state	root	ECP1	ECP2	EGP
$^{10}B_2$	1	0	0	0
$^{10}B_1$	1	9388	9700	9196
$^{10}A_1$	1	9845	9713	9199
$^{10}A_2$	1	11290	11491	11214
$^{8}A_1$	1	1304	1352	1320
$^{8}A_2$	1	9266		9320
$^{8}B_2$	1	9339		9323
$^{8}B_1$	1	10620	9798	11041
$^{6}B_2$	1	2584	2719	2653
$^{6}A_1$	1	9352	9879	9463
Δ_{av}		0	4.7%	2.1%

[a] In cm^{-1}.

2.2.2. The Novelty Accessible Thanks to EGPs. In the previous section, we have seen that the use of EGPs was efficient to reduce the size of the calculation. We shall prove later (section 4.1) that this reduction does not affect the quality of the calculation. Therefore, we shall have also the opportunity to evaluate the influence of a vibrational mode on the energy of the states, cf. section 4.4.

3. Methodological Details

3.1. Level of Calculation. The calculations without EGP were done using Gamess[17] (MRPT), and MOLCAS 5.2.[18] The ones with EGPs were carried out with MOLCAS 5.2 (CASSCF, CASPT2, CCSD).

In order to validate the EGP of NH_3, we have used two different ECPs on Fe and compared the results with the one obtained with the NH_3 EGP (section 2). The ECP1 is an ECP from Stuttgart[12] and associated basis, whereas ECP2 is an ECP by Krauss et al.[11]

All the calculations were carried out using Stuttgart[12,10] effective core potentials on Fe and O and associated basis. The basis on the H on the bridging OH was 3-21g.[19] The NH_3 effective group potential[1] is centered on the pseudo $N^{\#}$ atom. The basis on this atom is an uncontracted 1s2p basis. The s exponent is 1.7605965, and the 2 p exponents are 1.3760213 and 0.1346355. The EGP used was extracted during a previous work by Poteau et al.[2] Our CASPT2 calculations were done using the G3 Fock Hamiltonian[13] with an imaginary shift of 0.4. With these conditions, the weight of the reference wave function in the CASPT2 wave function appears to be the same for all the states we computed (ca. 74%). This weight is not as close as we expected, and this is probably due to the fact that we did not follow the recommendation cited in the previous section. Anyway, the fact that the weight was similar for each state allowed us to trust our calculations according to Persico.[20,21]

4. Results and Discussion

4.1. Validation of the EGP. The computation of the spectrum of the mixed valence molecule $[Fe_2(OH)_3(NH_3)_6]^{2+}$ requires us to treat properly the system in its ground state and excited states. Before we used the EGP to compute all the spectrum of the molecule, we made sure that the NH_3 EGP was not introducing a bias. In order to do so, we computed the lower states of each irreducible representation of the C_{2v} symmetry group at the CASSCF level with two kinds of ECP on the irons,[10,11] and we compared the results with the one obtained with EGP on NH_3. The results of this study are given in Table 2.

Table 3. Comparison of the Transitions[a] between CASPT2 (Using Either an ECP on the N Atoms[12] or an EGP to Model the NH_3 Ligand) and CCSD Calculations Using EGPs

state	CASPT2(ECP)	CASPT2(EGP)	CCSD(EGP)
$^{10}B_2$	0	0	0
$^{10}B_1$	9691	9426	9264
$^{10}A_1$	10289	9911	9270
$^{10}A_2$	11290	10308	11569

[a] In cm^{-1}.

As we expected, the difference between ECP and EGP calculation is of the same amplitude as the difference between two different ECPs. The mean difference between two sets of calculations *a* and *b* containing *n* values, the set *a* being considered as the reference, is computed this way: $\Delta_{av} = 1/n\sum_{i=1}^{n}|a_i - b_i|/a_i$. These values are computed taking the first column of Table 2 as reference. These values are more than encouraging. When one compares the first column and the third one, Δ_{av} is the error one does when one uses EGPs for NH_3. Since this error is of the same amplitude of the difference one obtains using two different ECPs, we can trust the results obtained with EGPs. We can say after this study that the problem is well reproduced with our NH_3 EGP at the CASSCF level. In other terms, we showed with this preliminary work that the occupied orbitals are well reproduced by our EGPs. No virtual orbital is involved in this test.

Another study will be done at the CASPT2 level to take into account the dynamic correlation, so the previous study is a first step but not a complete validation of the EGP. To validate it completely, we performed calculations with EGP including static and dynamic correlation. These calculations will validate the virtual orbitals we generate with the EGP. We compared three different calculations. The first one is a CASPT2 calculation with ECP only. This calculation was possible for the highest spin states of each symmetry since the size of the CASSCF space is small for these states. The second one is a CASPT2 calculation with EGP and the third one is a CCSD calculation using EGP. These three calculations (Table 3) will be referred to as *a*, *b*, and *c* until the end of this discussion. We compared CCSD and CASPT2 calculations using EGP arguing that these two methods use the virtual orbitals in two completely different ways.

The mean error between calculations *a* and *b* is 4.9% which is reasonable according to the CASSCF results. The agreement between *b* and *c* seems to indicate that the CASPT2 does reasonably well in reproducing the correlation. Once again[4] the quality of the EGP in the treatment of the dynamic correlation is shown. We can safely use the EGP to perform the calculation of the entire spectrum of the molecule with EGP.

4.2. The Equilibrium Geometry. The compound belongs to the D_{3h} symmetry group, but we will treat it in the first abelian subgroup available which is C_{2v}. This is due to the fact that no program to our knowledge can perform a CASSCF calculation in a symmetry group which is not abelian. The reason for that is the technical difficulties which would arise in such calculations.

Table 4. Correspondence between the Excitations between Orbitals and the Transitions between States in D_{3h} and C_{2v}

excitation		transition	
D_{3h}	C_{2v}	D_{3h}	C_{2v}
$a_1' \rightarrow e''$	$a_1 \rightarrow a_2$	$A_2'' \rightarrow E''$	$B_2 \rightarrow A_1$
	$a_1 \rightarrow b_2$		$B_2 \rightarrow B_1$
$a_1' \rightarrow e'$	$a_1 \rightarrow a_1$	$A_2'' \rightarrow E'$	$B_2 \rightarrow A_2$
	$a_1 \rightarrow b_1$		$B_2 \rightarrow B_2$
$a_1' \rightarrow a_2''$	$a_1 \rightarrow b_2$	$A_2'' \rightarrow A_1'$	$B_2 \rightarrow A_1$

Table 5. Degeneracies Expected in the C_{2v} Calculations Due to the D_{3h} Geometry of the Molecule

state symmetry C_{2v}	root number	D_{3h} symmetry
$^{10}B_2$	1	A_2''
$^{10}A_1$	1	E''
$^{10}B_1$	1	
$^{10}A_2$	1	E'
$^{10}B_2$	2	
$^{10}A_1$	2	A_1'
$^{10}A_2$	2	E'
$^{10}B_2$	3	
$^{10}A_1$	3	E''
$^{10}B_1$	2	

Table 6. Spectrum[a] at the CASSCF Level

state	energy (cm^{-1})	av energy (cm^{-1})
$^{10}B_2$	0	0
$^{10}B_1$	8559	8823
$^{10}A_1$	9088	
$^{10}B_2$	10333	10583
$^{10}A_2$	10833	
$^{10}A_1$	13786	13786
$^{10}A_2$	16737	17148
$^{10}B_1$	17559	
$^{10}A_1$	17826	17967
$^{10}B_2$	18108	

[a] The energies are given in cm^{-1}.

4.2.1. High Spin States ($2S + 1 = 10$). First of all, let us consider the transitions which are experimentally measurable, i.e., the ones which correspond to the transitions allowed by symmetry in D_{3h} from the high spin ($^9/_2$) ground state. For convenience we present in Table 4 the correspondence between the excitations between orbitals and the transitions between states in D_{3h} and C_{2v}. It is worth noting that the transitions $A_2'' \rightarrow E'$ are not allowed by symmetry in D_{3h} since the direct product $A_2'' \otimes E' = E''$ and E'' does not contain any component of the dipole moment. Table 5 shows the degeneracies expected in a C_{2v} study.

The CASSCF Spectrum. The spectrum given by the CASSCF calculation preceding the CASPT2 one (cf. Table 6) reveals that the degeneracies are the ones expected. Nevertheless, the four last states are not ordered properly, and their degeneracies are wrong, due certainly to small symmetry breaking, according to the previous section. We shall see in the next section that the introduction of the dynamic correlation by the CASPT2 method will correct this bias. It is worth pointing out that the CASSCF reproduces qualitatively the spectrum in the lower part but the high roots are not described correctly since the states are computed with average orbitals.

The CASPT2 Spectrum. The CASPT2 spectrum was computed (Table 7 with the G3 Fock Hamiltonian[13] which is known to give good results with transition metals. This spectrum respects the degeneracies of the D_{3h} point group and gives the proper order of the high states. This is a noticeable improvement in comparison with the CASSCF results. This is an argument for doing our next calculations at a higher correlated level than the CASSCF. This seems to indicate as well that the active−inactive correlation which is not taken into account by the CASSCF approach might play a role in the magnetic properties of the compound under interest.

Table 7. Spectrum[a] at the CASPT2 Level

state	energy (cm^{-1})	av energy (cm^{-1})
$^{10}B_2$	0	0
$^{10}B_1$	9463	9703
$^{10}A_1$	9943	
$^{10}B_2$	10006	10160
$^{10}A_2$	10315	
$^{10}A_1$	13253	13253
$^{10}A_2$	18635	18876
$^{10}B_2$	19117	
$^{10}B_1$	19233	19478
$^{10}A_1$	19723	

[a] The energies are given in cm^{-1}.

Table 8. Comparison between the Spectra[a] 3 at the CASSCF and CASPT2 Level with EGP[b], the DFT Approach,[5] and the Experimental Data[15]

transition D_{3h}	DFT	CASSCF	CASPT2	CCSD	exptl
$^{10}A_2'' \rightarrow {}^{10}E''$	8388	8823	9703	9267	
$^{10}A_2'' \rightarrow {}^{10}E'$	10987	10583	10160	11569	7380
$^{10}A_2'' \rightarrow {}^{10}A_1'$	13660	13786	13253		13500
$^{10}A_2'' \rightarrow {}^{10}E''$	22712	17148	18876		17860
$^{10}A_2' \rightarrow {}^{10}E'$	21207	17967	19478		21350

[a] The energies are given in cm^{-1}. [b] This work.

Comparison with DFT and Experiment. In a previous paper, Barone et al. did a study on the same mixed valence compound with a DFT approach.[5] In this study they did an open shell DFT calculation. Since this method does not allow them to compute the electronic states as we did, they computed the spectrum using the Slater transition state theory.[14] It is worth noting that using this method one assumes that the orbitals are unchanged between the two states. In Table 8, the CASPT2 calculations were done using the multistate approach; i.e., the states were computed with average orbitals at the CASSCF level and uncoupled in the CASPT2 calculation. As we can see our results stick to the experiment except for the first transition. This behavior appears also at every level of calculation which indicates that our EGP is not guilty of this behavior. The CASSCF results are in good agreement with experiment, and the active−inactive correlation included via CASPT2 does not seem to be crucial. Nevertheless, we shall see later that this is no more true for the lower spin states. It is to be noted that the CASSCF method shows a deterioration of its quality for the higher roots. The inversion of the two last transitions which appear in the DFT approach does not appear with CASPT2. This is probably due to the fact that the DFT approach makes the approximation that the orbitals do not change when a transition occurs. Such an approximation

might be good for the first states but becomes more and more approximate for the higher excitations. Since in the multistate CASPT2[22] approach each state is computed in its own orbitals, this problem disappears.

4.2.2. The Low Spin States. As stated earlier, it is possible at the CASSCF + CASPT2 level to compute the entire spectrum of the mixed valence compound we are studying thanks to EGPs. In their article, Barone et al. were regretting that their approach had to rely on a spin Hamiltonian formalism and had the ambition to develop a methodology to get rid of this. According to them, this would lead to a validation of the spin Hamiltonian formalism itself. We will see later that this is true to some extend. The EGPs relieved us to use the spin Hamiltonian formalism by computing each multiplet structure by itself. In order to do so, we computed the lower roots in each symmetry available for each $S = \{^9/_2, ^7/_2, ^5/_2, ^3/_2, ^1/_2\}$. Within the DFT approach, it is not possible to compute the states with spin different from $^9/_2$ (we are not talking about TDDFT here). Barone et al. managed to compute the exchange coupling constant J using broken symmetry approach. Then with the B constant they obtain from the difference between the two $S = ^9/_2$ states, they predicted the energies of the lower spin states using eq 1. The results we obtained for the spectrum of the low spin states will be presented in two parts. At first we will present our CASSCF results. We will plot the CASSCF spectrum and the spectrum we generated with eq 1 using the CASSCF states (($^9/_2$, −), ($^9/_2$, +), ($^7/_2$, −)) to get a B and J constant [$B = (E(^9/_2, +) - E(^9/_2, -))/10$; $J = (E(^9/_2, -) - E(^7/_2, -) - B)/9$]. In a second step we shall do the same for the CASPT2 spectrum. This approach will allow us to see the influence of the dynamic correlation on the spectrum and check if the utilization of eq 1 is still suitable for the system under study.

The CASSCF Spectrum: The Static Correlation. Our CASSCF wave functions were obtained using 10 active orbitals and 11 electrons section 2.1.2. In order to treat all the d orbitals in an identical manner, we chose to compute these states in the average orbitals over the 3 first states of each symmetry. [For the states ($^1/_2$, ±), we had to depart from this rule since the CASSCF algorithm did not converge with 3 states but only with 2 states.] This choice became ours after we realized that the calculation done in C_{2v} was introducing a bias which was a symmetry breaking in the molecular orbitals. In D_{3h} the d_{z^2} on one side and the $d_{x^2-y^2}$ and d_{xy} orbitals on another side belong to different symmetry and are not allowed to mix. This is no more the case in the C_{2v} point group in which these orbitals belong to the same symmetry. This leads to an artificial mixing of these orbitals. We can avoid it by doing an average calculation on different states so that the average occupation of the average d orbitals are of the same order. Thus, the wave function keeps its D_{3h} symmetry. It worth noting that this problem has a tendency to be stronger as the total spin S increases. This is due to the fact that the number of configurations is very low [there are 3 configurations implied in the states $S = ^9/_2$] so the dissymmetry is emphasized. The spectrum obtained at the CASSCF level is presented in Table 9. This spectrum and

Table 9. CASSCF Spectrum Obtained[a]

state	CASSCF	formula
+9/2	13786[b]	13786
$+^7/_2$	12186	11941
$+^5/_2$	10530	10200
$+^3/_2$	8897	8563
$+^1/_2$	6938	7029
$-^1/_2$	4001	4272
$-^3/_2$	3181	3049
$-^5/_2$	1986	1929
$-^7/_2$	913[b]	913
$-^9/_2$	0[b]	0

[a] The energies are given in cm^{-1}. The results given by the formula are obtained with $B = 1379$ and $J = 103$. [b] Values used to extract B and J (cf. section 4.2.2).

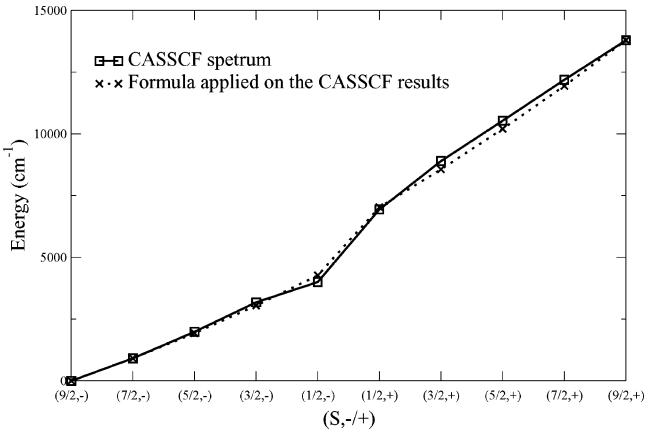

Figure 3. CASSCF spectrum compared to the results given by eq 1.

the one generated by eq 1 using the B and J parameters calculated with the CASSCF states are plotted in Figure 3. The CASSCF results are in perfect agreement with the one predicted by the formula. Furthermore, the values of B and J compare very well with experiment which gives $B = 1350$ cm^{-1} and a superior bound of $|J| > 140$ cm^{-1}. These results show clearly that the spin Hamiltonian formalism is validated by the CASSCF approach. This means that this formalism takes entirely into account the valence correlation. Let's analyze the occupation number of the linear combination of the d_{z^2} orbitals. In the 10 states we are interested in, the total number of electrons in the bonding and antibonding molecular orbitals is 3. From a formal point of view, one would expect 2 electrons in the bonding orbital for the (S, −) states and 1 electron in the antibonding one. The occupations should be inverted in the (S, +) states. This strict behavior is observed for the $^9/_2$ states because these states are built on one configuration. Since for the other values of S the number of configurations on which the states are constructed becomes higher as S decreases, the extra electron is more and more delocalized between the two molecular orbitals arising from the d_{z^2} orbitals of the metallic centers. Thus, the variation of the occupation number of the bonding orbital should decrease as S decreases for the (S, −) states. The occupation number of the antibonding orbital should show the exact opposite variation; i.e., its occupation should increase as S increases for the (S, +) states and the amplitude of this variation should be of the same order of the preceding one. Figure 4 shows the variation of the occupation of the

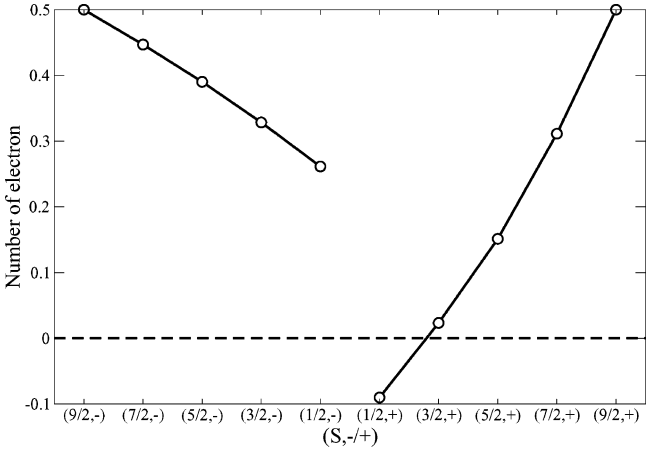

Figure 4. Excess of electron compared with 1.5 in the bonding (antibonding) molecular orbital for the (S, $-$) ((S, $+$)) CASSCF states.

Table 10. CASPT2 Spectrum Obtained[a]

state	CASPT2	formula	DFT
$+^9/_2$	13253[b]	13253	13660
$+^7/_2$	12718	11669	11704
$+^5/_2$	12935	10141	9856
$+^3/_2$	11984	8672	8144
$+^1/_2$	10841	7260	6570
$-^1/_2$	6649	4609	3882
$-^3/_2$	4436	3370	2668
$-^5/_2$	2578	2189	1642
$-^7/_2$	1066[b]	1066	752
$-^9/_2$	0[b]	0	0

[a] The energies are given in cm^{-1}. The results given by the formula are obtained with $B = 1325$ and $J = 58$. [b] Values used to extract B and J (cf. Sec. 4.2.2).

bonding and antibonding orbitals for the (S, $-$) and (S, $+$) states, respectively. To these occupation numbers we have subtracted 1.5. This allow us to know if at least half of the 3 electrons occupying the d_{z^2} orbitals are on the molecular orbital which is expected to be doubly occupied. As we can see, the variation of the occupation number is more important in the case of the (S, $+$) states than in the (S, $-$) states. Furthermore, the most striking thing is that for the $+^1/_2$ state the occupation of the antibonding orbital is lower than 1.5. This means that, contrary to what one would expect, the extra electron did not formerly jump on the antibonding molecular orbital. It is worth noting that this behavior is not taken into account by the spin Hamiltonian formalism. In the formal approach, one would expected to have 2 electrons in the bonding orbital in the five first states and a double occupation of the antibonding orbital for the (S, $+$) states.

The CASPT2 Spectrum: The Dynamical Correlation. In order to compare our results obtained at the DFT level and with experiment, we did a CASPT2 treatment on top of the CASSCF results presented above. Since the CASSCF wave functions were obtained in average orbitals, we have used the CASPT2 multistate algorithm in order to avoid the mixing of these states at the correlated level. Thus, we obtained a different set of orbitals for each states. The CASPT2 results are presented in Table 10. Figure 5 presents the CASPT2 results and the spectrum given by application of eq 1 with the B and J extracted from the CASPT2

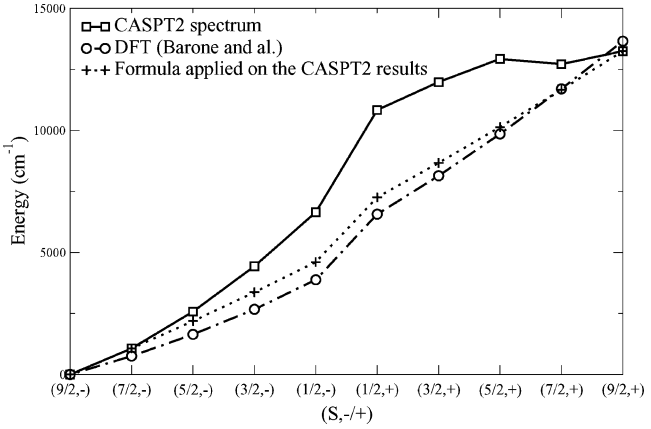

Figure 5. CASPT2 spectrum compared to the results given by eq 1 and the results given in a previous work by Barone et al.[5]

energies. In this figure, we also introduced the spectrum generated by application of eq 1 with B and J obtained with the broken symmetry approach.[5] The CASPT2 results no longer follow the behavior predicted by the spin Hamiltonian formalism. The difference is more important for the states {($^1/_2$, $+$), ($^3/_2$, $+$), ($^5/_2$, $+$)}. This seems to indicate that the influence of the active−inactive correlation introduced by the CASPT2 approach is no longer negligible for these states. The value of B end J still compare very well with experiment ($B = 1350$ cm^{-1} and $J \leq 140$ cm^{-1}). Nevertheless, since the experimental values of B and J are computed with the help of eq 1, they cannot reflect the disagreement that we observe. The occupation numbers of the CASPT2 d_{z^2} natural orbitals are very similar to the ones obtained at the CASSCF level presented in Figure 4. For the states {($^1/_2$, $+$), ($^3/_2$, $+$), ($^5/_2$, $+$)}, the population on the antibonding orbital is lower than the lowest occupation number for the (S, $-$) states. This obviously means that the transfer of the extra electron from bonding to antibonding orbitals is energetically unfavorable. This feature brought by the active−inactive correlation is not included in the spin Hamiltonian formalism. Since the influence of the core is not taken into account at all by the spin Hamiltonian, it is understandable that the correlated results do not behave like eq 1 would predict. As a summary, we could say that the most striking thing is the very good behavior of the formula for predicting the CASSCF spectrum. On the contrary, that it fails to match the CASPT2 results is not surprising. As a matter of fact, eq 1 is based on the assumption that the electronic configurations on which the states are built arise from some of the many possible arrangement of the electrons in the magnetic orbitals. In our example, the configurations arise from the arrangement of the 11 electrons in the 10 linear combinations of the d orbitals of the irons. This is precisely what the CASSCF wave function consists of. On the other hand, this model does not take into account others excitations which would modify the wave function. This is exactly what the CASPT2 approach allow us to do. Note that in the CASPT2 wave functions we obtained the weight of the reference function (i.e., the CASSCF one) which is about 74%. This means that the modification of the wave function by the excitations which were not taken into account formerly is not negligible. This

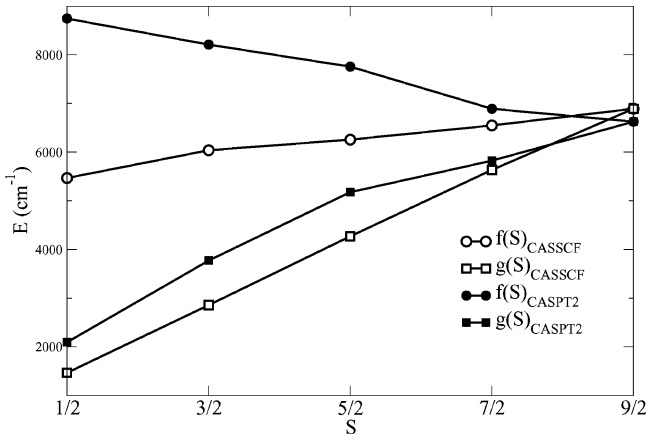

Figure 6. Values of $E(S,+) + E(S,-)/2$ and $E(S,+) - E(S,-)/2$ in terms of S for the CASSCF and CASPT2 calculations. These data were fitted (see text). The fitting curves are not presented on the graph to avoid overloading it.

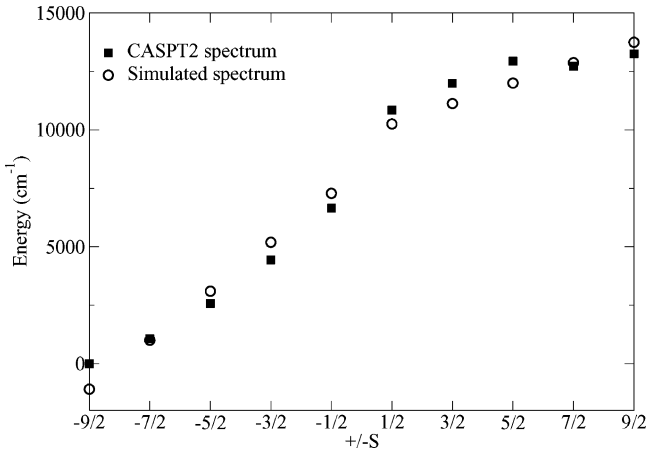

Figure 7. Comparison of the actual CASPT2 spectrum and the one obtained by the fitting procedure.

explains why the CASPT2 spectrum we obtained does not follow eq 1 while the CASSCF one is in a very good agrement with it.

4.3. A Model for the CASPT2 Results. As shown in the previous sections, eq 1 does not appear to be reliable for the study of the spectrum. This formula is based on two assumptions that we shall keep in eq 2. There are two terms, the first one, $f(S)$, corresponding to transitions in which spin changes and the other one, $g(S)$, which takes into account the localization of the electron on one or the other metallic center. There's also a constant, K, which gives the origin of the energy.

$$E(S, \pm) = f(S) \pm g(S) + K \tag{2}$$

From eq 2 we can derive the functions $f(S)$, $g(S)$ by the fit of the formulas given in eqs 3 and 4. The constant K, which is a shift of the energy, will be skipped during the following study.

$$f(S) = \frac{E(S, +) + E(S, -)}{2} \tag{3}$$

$$g(S) = \frac{E(S, +) - E(S, -)}{2} \tag{4}$$

The functions $f(S)$ and $g(S)$ were extracted by fits on the curves presented in Figure 6. The fitting for the CASSCF results is not problematic as expected since these data were already given by eq 1. The functions obtained for the CASSCF spectrum are given here. Note that we tried to put the following functions in a form close to the one expected by eq 1 when this did not spoil the correlation coefficient.

$$f(S)_{\mathrm{CASSCF}} = 53S(S + 1) \text{ (corr} = 0.9873)$$

$$g(S)_{\mathrm{CASSCF}} = 1400(S + {}^1/_2) \text{ (corr} = 0.7998)$$

The functions obtained for the CASPT2 spectrum are given here. Note that in the CASPT2 case we did not manage to write $f(S)$ in a form close to the one given by eq 1. This is understandable since the signs of the coefficient in front of the quadratic and the linear term in S are different.

$$f(S)_{\mathrm{CASPT2}} = 9S^2 - 601S \text{ (corr} = 0.7925)$$

$$g(S)_{\mathrm{CASPT2}} = 1483(S + {}^1/_2) \text{ (corr} = 0.7844)$$

There are two main features that one can extract from these fitting procedures. The first one is the fact that the $g(S)$ function has the same linear coefficient in S; about 1400 cm^{-1}. This means that the delocalization is not drastically modified by the introduction of the active−inactive correlation. The second one is the large modification of the behavior of $f(S)$ from CASSCF to CASPT2. As a matter of fact the values of $f(S)$ increase with S for the CASSCF values and decrease with S when one introduces the CASPT2 treatment. This means that the compound is expected to be ferromagnetic at the CASSCF level and antiferromagnetic at the CASPT2 level of calculation. This is a major change in the physics of the molecule of interest. Figure 7 shows the spectrum generated by the $f(S)$ and $g(S)$ obtained for the CASPT2 results. The comparison of Figures 5 and 7 shows clearly an improvement of the predicted spectrum when one uses the fitted functions instead of the results obtained via eq 1. If one looks closely at the functions we used, the main difference between eq 1 and the fitted ones is the dependence of the superexchange part (i.e., the J part in eq 1 or the $f(S)$ function in the fit procedure). The spin Hamiltonian formalism expects this part to have the same coefficient for the linear and quadratic terms in S. This is no more true in our case when we introduce the active−inactive correlation. In fact, this is not very surprising; ab initio calculations on small systems[25] have already shown that there are effects to take into account beyond double exchange which are not taken into account by formula 1. Our calculations allow us to quantify these effects. Our results show clearly that the dynamical correlation, which is usually assumed to be a small correction, is no more negligible in our case. Our results indicate a strong variation of this part in terms of S in a linear manner. The variation of the parameter in front of the

(25) de Loth, Ph.; Cassaux, P.; Daudey, J.-P.; Malrieu, J.-P. *J. Am. Chem. Soc.* **1981**, *103*, 4007.

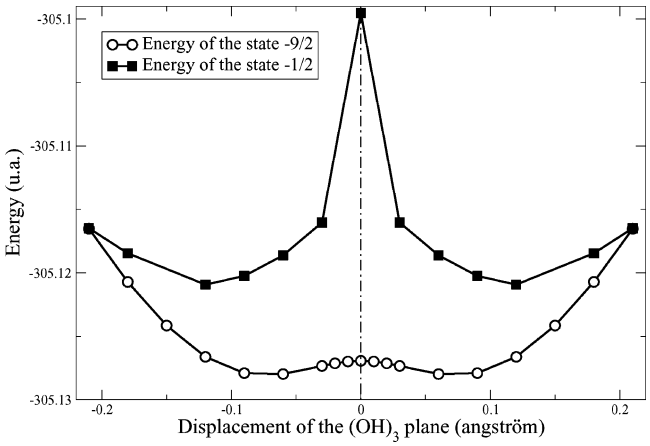

Figure 8. Variation of the energy of the states $-^1/_2$ and $-^9/_2$ in terms of the displacement of the $(OH)_3$ plane.

linear variation in S varies by about 1000 cm^{-1}, and more important, it changes sign. This change is very important for the attribution of a ferro- or antiferromagnetism to the compound of interest.

4.4. The Influence of a Vibrational Mode. 4.4.1. The Low States. The former study was suitable for a D_{3h} geometry. Nevertheless, this static [i.e., fixed geometry] approach is not sufficient for the characterization of the mixed valence compound as a localized or delocalized compound. In order to determine this, we followed the proposition of Barone et al.[5] to take into account a special vibrational mode. On the basis of work of Blondin and Girerd,[16] Barone et al. propose to approximate the influence of the out-of-phase combination of the breathing motions on the two monomeric subunits. This vibration consists of the reduction (or augmentation) of three Fe−N distances and the augmentation (respectively, reduction) of the three other Fe−N distances on the other side of the molecule. In the same time, the $(OH)_3$ plane moves along the Fe−Fe axis. This last movement is the main component of the vibration. In order to evaluate the influence of this vibrational mode on the localization of the extra electron on one metallic center, we computed the energy in terms of the displacement of the $(OH)_3$ plane. In our calculation, we did not relax the geometry of the molecule. This study was done in the C_s point group of symmetry. In order to conserve as much as possible the C_{3v} symmetry of the wave function, we averaged the CASSCF calculation on 6 states using the same argument than formerly and uncoupled the 3 lowest in the multistate CASPT2 calculation. According to Kahn,[7] among the 10 states at our disposal, only the five lowest may show a localized behavior. Among these states, the $-^9/_2$ and the $-^1/_2$ are the more extreme ones. Indeed, the $-^9/_2$ state is expected to be delocalized which means that the energy in terms of the displacement of the $(OH)_3$ plane should be a well centered at the center of the Fe−Fe bond. On the other hand, the energy of the $-^1/_2$ state should have the shape of a double well connected via a barrier whose height is the thermal energy required by the extra electron jumping from one metallic center to the other one. Figure 8 shows the potential energy curves of the $-^9/_2$ and $-^1/_2$ states. Indeed, these two states show a localized behavior. The values of the energetic barrier are found to be roughly 4200 and 350 cm^{-1} for the $^1/_2$ and $^9/_2$ states, respectively. In order to analyze these results, we have built an effective Hamiltonian which takes explicitly into account the displacement of the $(OH)_3$ plane, Δr, the variation of the energy λ of the occupied orbital, and k the force constant associated to the movement of the plane. The extra diagonal element of this Hamiltonian is noted β. Following the same reasoning than Blondin and Girerd, we obtain the following form of the energy for the lower state:

$$E = \frac{k\Delta r^2}{2} - \sqrt{(\lambda\Delta r)^2 + \beta^2} \tag{5}$$

This equation can be rewritten in terms of the dimensionless variable $q = (\lambda/k)\Delta r$.

$$E = \frac{1\lambda^2}{2\,k}q^2 - \sqrt{\left(\frac{\lambda^2}{k}q\right)^2 + \beta^2} \tag{6}$$

Before going further we define $E_{op} = \lambda^2/k$ as the energy between the minimum of a well for a $(S, -)$ state and the curve of the corresponding $(S, +)$ state at the same Δr. We define also E_θ as the height of the energetic barrier between the two wells of a potential energy curve. The form of E_θ can be written as follows:[16]

$$E_\theta = \frac{1}{4}E_{op} + \frac{\beta^2}{E_{op}} - |\beta| \tag{7}$$

The results we obtained for the $^1/_2$ states are $E_\theta = 4694$ cm^{-1} and $E_{op} = 8886$ cm^{-1}. With these values, we obtain $|\beta| = 2015$ cm^{-1}. These values are consistent with the fact that the $(S, -)$ state is localized if and only if $E_{op} > 2|\beta|$. At this point, it is worth noting that the value of E_{op} that we extracted from our results was calculated between the bottom of the well for the $-^1/_2$ state and the energy of the $+^1/_2$ state. This gives us an approximate value for E_{op} which might be underevaluated. With the value of β we are able to compute the different B constants if one agrees on the fact that the $g(S)$ function should vary like $B \times (S + ^1/_2)$. Then for $S = ^1/_2$, $B = \beta$. So with this approach we found a value for the B constant which is compatible with the B we obtained from the former approach (about 1325 cm^{-1}, cf. Table 10). It is worth noting that $\beta(^1/_2)$ differs from B because they were obtained by two different ways. B was extracted by using the model Hamiltonian eq 1 on our CASPT2 results (Table 10) whereas $\beta(^1/_2)$ was obtained by fitting the curves 8 using eq 6. The most important result when one compares these two numbers is that they have the same order of magnitude. We should remember that this value is an upper limit according to the fact that E_{op} was underestimated. Nevertheless, we can build the energy potential curves by choosing an average β to be 1650 cm^{-1} and by re-evaluating E_{op} at 11000 cm^{-1}. The increase of E_{op} is based on the fact that the E_{op} we obtained by the former study was underestimated. The correction is taken to be half of the value of E_θ which is reasonable. The value of E_θ obtained with these parameters

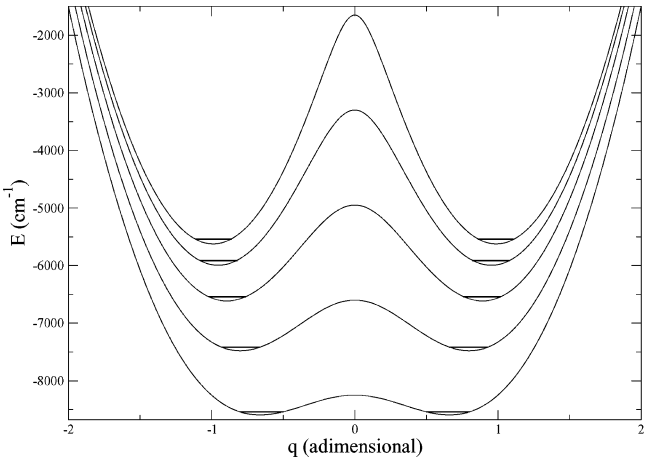

Figure 9. Potential energy curves of the 5 lower states obtained with $\beta = 1650$ cm^{-1} and $E_{op} = 11000$ cm^{-1}. q is the adimensional variable such as $q = (\lambda/k)\Delta r$. The energy of the first vibrational states are plotted in bold lines for each curve.

is found to be around 400 cm^{-1} which is totally compatible with the barrier we found formerly for this state.

4.4.2. The Influence of the Zero Point Energy. Now that we have parameters extracted after taking into account the influence of this vibration, we shall generate the spectrum with all the states. In order to do so, we have generated the energy potential curves of the states where the extra electron is on the low energy orbital, see Figure 9. These curves show clearly that our results extracted from the $^1/_2$ states are compatible with a localization of the $-^9/_2$ state. By finding the solutions of the vibrational problem, we were able to compute the spectrum taking into account the zero point energy, i.e., the energy of the first vibrational mode. It turns out that for the ground state of the molecule in its first vibrational mode, this state is localized. Indeed, its energy 291 cm^{-1} is lower than the height of the barrier 344 cm^{-1}. This result has to be considered carefully since the difference between the top of the barrier and the vibrational mode is no more than 50 cm^{-1}. This result seems to disagree with the experimental results[15,6] which show clearly that this compound has a delocalized ground state. Nevertheless the small energetic barrier which appears in our results could be attributed to a small symmetry breaking artifact which is well-known to appear in metallic dimer calculations.[26] This point is true for the ground state but no more true for the states $(S, -)$ with $S \in {}^7/_2; {}^5/_2; {}^3/_2; {}^1/_2$ which are clearly localized. This result reinforces the idea that the complex is delocalized in its ground state. On the other hand, the state $-^1/_2$ is localized as shown on Figure 9. With the inclusion of the zero point energy, the spectrum we obtained reproduces properly the experimental results, i.e., the transition between the states of spin $^9/_2$. This transition is about 13500 cm^{-1} experimentally and is found to be 16914 cm^{-1} which is a good result according to the fact that the potential energy curves were built without relaxing the geometry of the molecule while moving the $(OH)_3$ plane.

(26) Malrieu, J.-P.; Daudey, J.-P. *Strategies and Applications in Quantum Chemistry*; Ellinger, Y., Defranceschi, M., Eds.; Klüwer Academic Publishers: Norwell, MA, 1996; Vol. 103.

5. Conclusion

The effective group potential approach has been successful in order to compute the excited states of the mixed valence compound of interest. This approach was found more valuable than the broken symmetry approach since the computation of the entire spectrum of the molecule was possible at a high level of correlation. Moreover the calculations performed in this work allowed us to emphasize the deviations of the actual spectrum obtained with ab initio calculations from the predictive eq 1.

Last, we proposed a reformulation for the function which predicts the magnetic spectrum which fits our results. It shows clearly that this is the superexchange term which is the most sensitive to the dynamical correlation. We also investigated the vibrational mode which acts on the localization of the extra electron. The potential energy curves were obtained for two states, and the results we obtained allowed us to predict the behavior of all states in between. Then we have been able to take into account the zero point energy. These results allowed us to find transition energies similar to the experimental results. They also show the localization of all the $(S, -)$ states with the exception of the ground state for which the barrier found is so small that it is attributed to a small symmetry breaking. This compound is then found to belong to class III[23] in accordance with the experimental results obtained earlier.[15,6] This work is encouraging for the future of the EGPs in the investigation of high spin states. In the future we plan to extract an EGP for the tmtacn ligand and to do the study again in order to determine the impact of the replacement of this ligand with NH_3.

Acknowledgment. The authors would like to thank Franck Jolibois for discussions about the mixed valence compound and Nathalie Guihery and Jean-Paul Malrieu for valuable discussions about the deviations of the CASPT2 spectrum.

Supporting Information Available: Data from *Molcas*. This material is available free of charge via the Internet at http://pubs.acs.org.

IC034716H